Electronic Supplementary Information (ESI) for Chemical Communications. This journal is (c) The Royal Society of Chemistry 2025. Electronic Supplementary Information (ESI)

Zn-thiocatecholate functionalized MOF modified separator stabilizing zinc anodes for long-life aqueous zinc-ion batteries

Hujing Zhou,[‡a] Ruwei Chen,[‡a] Zhixin Jiang,[a] Jiangtao Li,[a] Hongyuan Liang,[a] Lai-Hon Chung,[a] Xuanhe Hu*[ab] and Jun He*[ab]

[a] School of Chemical Engineering and Light Industry, Guangdong University of Technology, Guangzhou 510006, P. R. China.
[b] Guangdong Provincial Laboratory of Chemistry and Fine Chemcial Engineering Jieyang Center, Jieyang 515200, P. R. China.
‡ These authors contributed equally to this work
E-mail: huxh@gdut.edu.cn, junhe@gdut.edu.cn

Experimental section

Synthesis of UiO-66

UiO-66 was synthesized following the previously reported procedure.[1] 2.5 mmol $ZrCl_4$ (583 mg) and 2.5 mmol 1,4-benzenedicarboxylic acid (H_2BDC) (415 mg) were dissolved in 30 mL *N, N*-dimethylformamide (DMF). Then, the mixture was heated at 120 °C for 24 h. After the reaction was completed, the product was collected by filtration, followed by washing with DMF and ethanol and drying in a vacuum oven at 60 °C for 12 h.

Synthesis of UiO-dcbdt-Zn

UiO-dcbdt was synthesized following previously reported procedures.[2, 3] The reaction of 1,4-dicarboxylbenzene-2,3-dithiol (H_2dcbdt) (0.214 mmol) with $ZrCl_4$ (0.17 mmol) led to the precipitation of UiO-dcbdt. The activated UiO-dcbdt (50 mg) was immersed in 1M aqueous $Zn(OAc)_2$ solution (40 mL), and stirred at room temperature for 72 h to yield UiO-dcbdt-Zn, replacing the solution with fresh every day. The powder was collected by filtration, washed several times with H_2O to ensure removal of solvent molecules, and then the collected product was dried under vacuum at 60 ℃ for 12h.

Fabrication of modified separator

The MOF modified separator was fabricated by vacuum filtration method. For example, 9 mg UiO-dcbdt-Zn and 1.0 mg polyvinylidene fluoride were first dispersed into 10 mL 1-methyl-2-pyrrolidinoneby ultrasonic vibration.[4] Then, vacuum filtration was performed to uniformly load the UiO-dcbdt-Zn onto the glass fibers separator. After drying at 60 °C for 12 h, the UiO-dcbdt-Zn modified separator with an areal loading of 0.50 mg cm^{-2} was obtained. UiO-66 modified separator were prepared by a similar procedure starting with UiO-66 in place of UiO-dcbdt-Zn.

Characterization

X-ray diffraction pattern was recorded on an X-ray powder diffractometer under Cu Kα radiation (λ = 1.54056 Å, 40 kV, 15 mA) with a scanning rate of 10° min^{-1} (Rigaku SmartLab). Fourier transform infrared spectrometry was performed using a spectrometer (Nicolet iS50R). The morphologies of the samples were examined by scanning electron microscopy (Hitachi 4300N). The cycling measurement was carried

out on a battery tester (Neware BTS-CT-3008-TC). Electrochemical impedance spectroscopy test was performed on a workstation (Donghua DH7006) in the frequency from 100 kHz to 0.01 Hz with an amplitude of 10 mV.

Electrochemical Measurements

Zn||Zn symmetric cells and Zn||Cu asymmetric cells were constructed using 2 M $ZnSO_4$ aqueous solution as the electrolyte and the Whatman glass fiber as the separator. For the preparation of Zn||MnO_2 full cells, α-MnO_2 electrode and 2 M $ZnSO_4$ + 0.1 M $MnSO_4$ aqueous solution were adopted as cathode and electrolyte, respectively. The slurry consisted of 70 wt% α-MnO_2, 20 wt% Ketjen black and 10 wt% PVDF was coated onto the carbon cloth to obtain the cathode. The mass loading of α-MnO_2 was controlled at 1.0~1.2 mg cm^{-2}. Galvanostatic charge/discharge and cycling tests were performed on a Neware automatic battery tester. Cyclic voltammetry (CV), chronoamperometry (CA), Electrochemical impedance spectroscopy (EIS) and Tafel data were recorded on a DH7006 electrochemical workstation.

Theoretical Calculations

The theoretical calculations employed the Vienna Ab-inito Simulation Package (VASP).[5, 6] The generalized gradient approximation (GGA) method with Perdew-Burke-Ernzerhof (PBE) functional is used to describe the exchange-correlation effects.[7, 8] The core-valence interactions were accounted by the projected augmented wave (PAW) method.[9] The energy cutoff of the plane-wave basis was set to 400 eV. The 3×3×1 k-points were selected to sample the Brillouin zone integration. The structural optimization was completed for energy and force convergence set at 1.0×10^{-4} eV and 0.02 eV $Å^{-1}$, respectively. The adsorption energy (Eads) was calculated by

$$E_{ads} = E_{total} - E_{Zn^{2+}} - E_{sub}$$

where E_{ads} is the calculated energies after the adsorption of Zn^{2+} on the substrates, $E_{Zn^{2+}}$ is the calculated energy of adsorbent, and E_{sub} means the calculated energy of UiO-66 or UiO-dcbdt-Zn surface.

Supplementary Figures

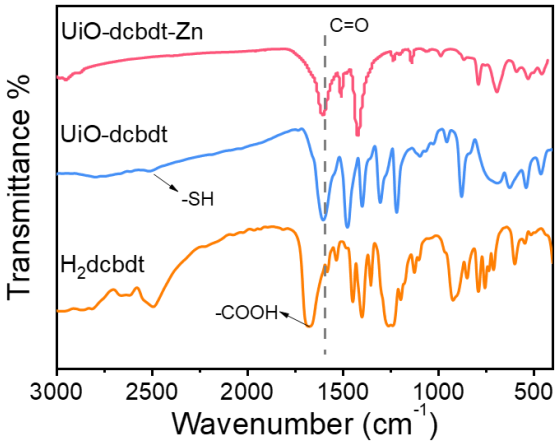

Figure S1. FT-IR spectrum of UiO-dcbdt-Zn, UiO-dcbdt and H_2dcbdt.

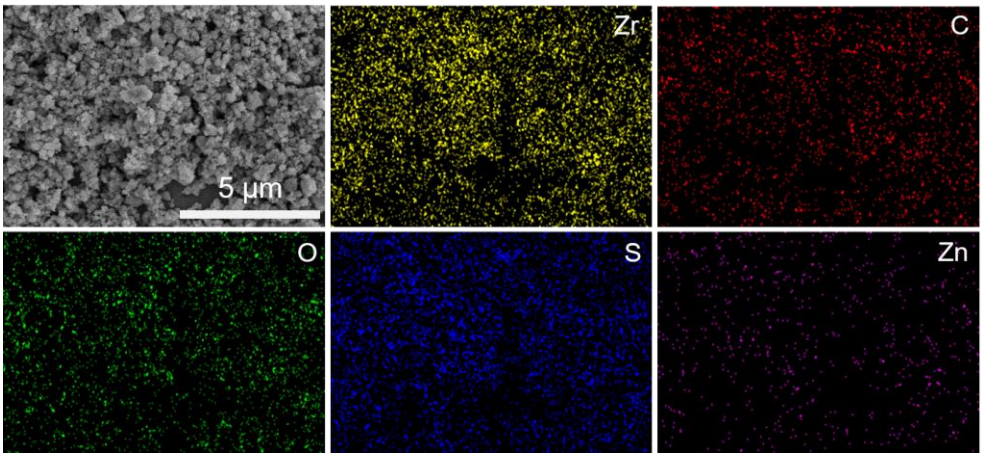

Figure S2. SEM images and EDS mapping of UiO-dcbdt-Zn.

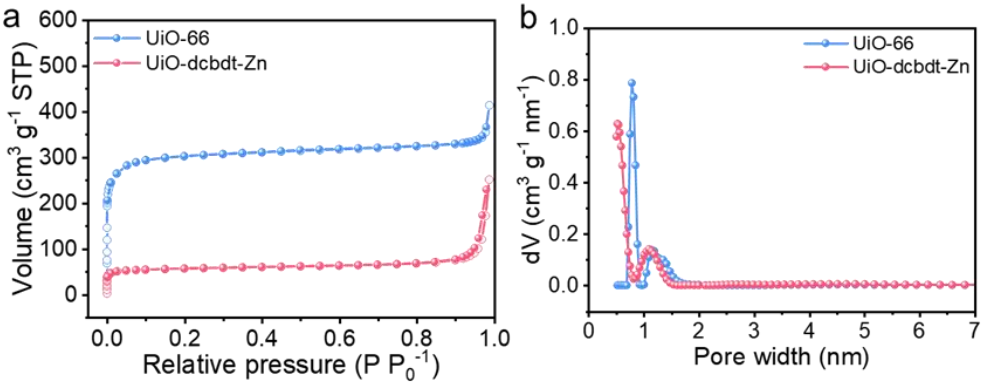

Figure S3. (a) N_2 adsorption isotherms and (b) pore size distribution curves of UiO-66 and UiO-dcbdt-Zn.

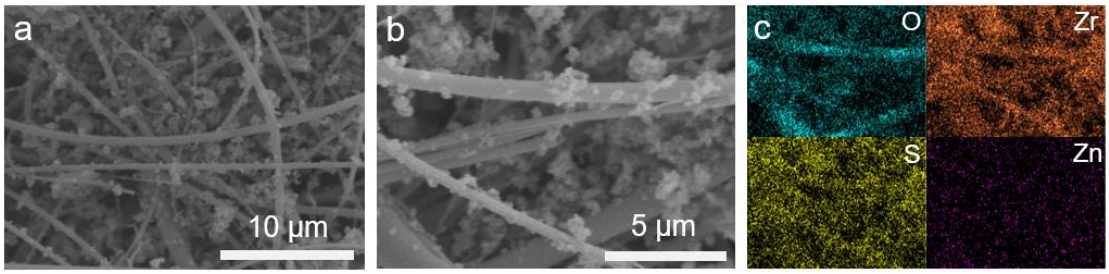

Figure S4. (a, b) SEM images and (c) EDS mapping of UiO-dcbdt-Zn@GF.

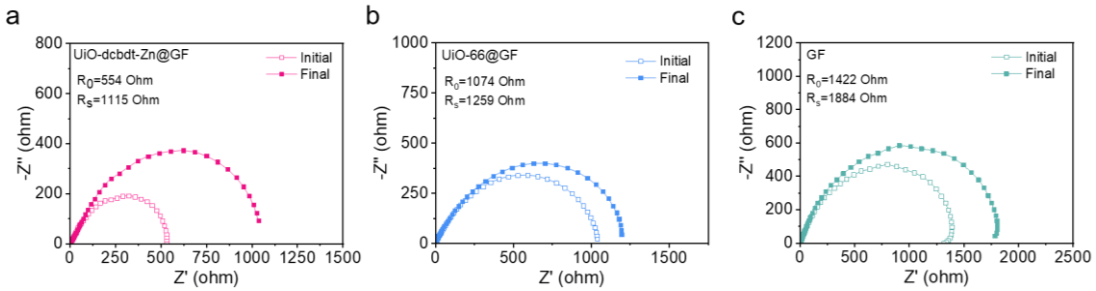

Figure S5. Nyquist plots of symmetric cells with (a) UiO-dcbdt-Zn@GF, (b) UiO-66@GF and (c) GF before and after CA measurement.

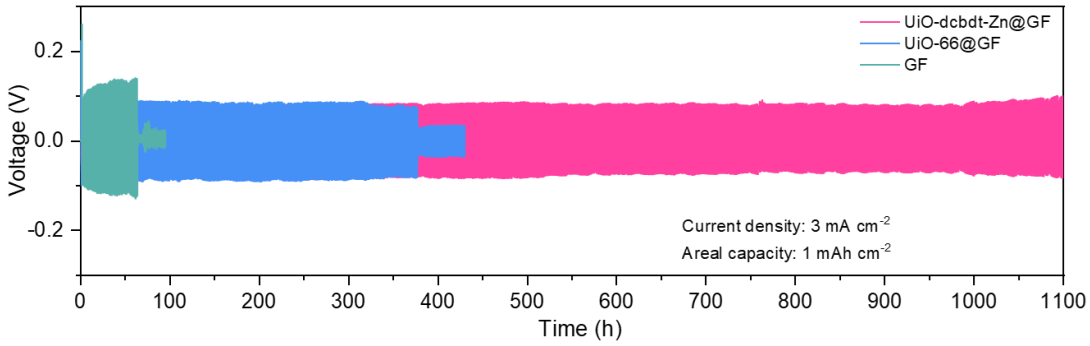

Figure S6. Cycling stability of Zn||Zn symmetrical cells using different separators at 3 mA cm^{-2}, 1 mA h cm^{-2}.

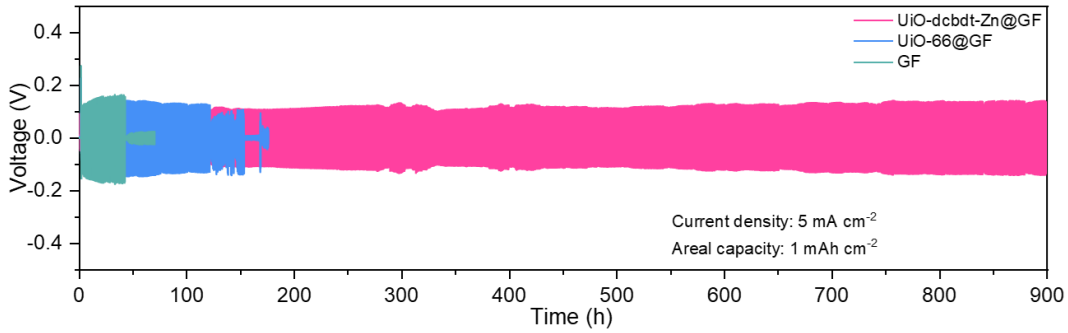

Figure S7. Cycling stability of Zn||Zn symmetrical cells using different separators at 5 mA cm^{-2}, 1 mA h cm^{-2}.

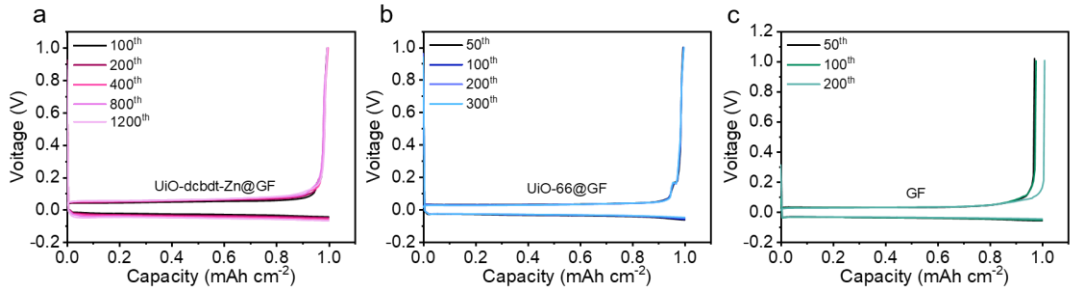

Figure S8. Voltage profiles of Zn||Cu cells with (a) UiO-dcbdt-Zn@GF, (b) UiO-66@GF and (c) GF at selected cycles.

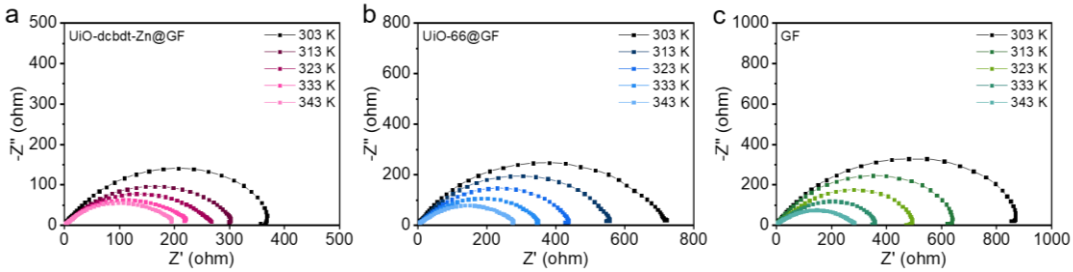

Figure S9. Nyquist plots of Zn||Zn cells with (a) UiO-dcbdt-Zn@GF, (b) UiO-66@GF and (c) GF at different temperatures.

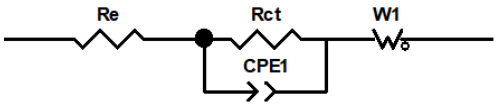

Figure S10. Equivalent electrical circuit of the EIS spectra.

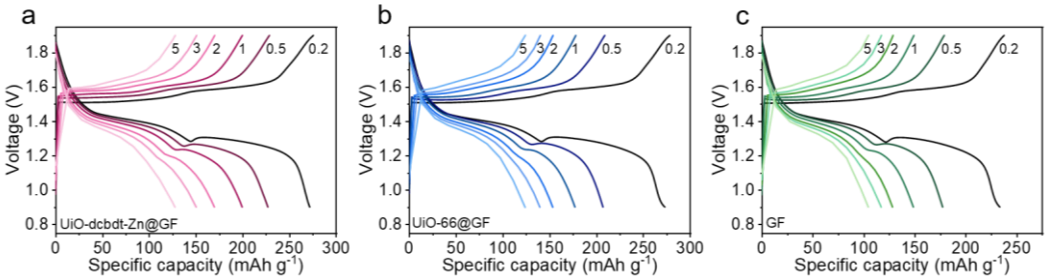

Figure S11. The charging/discharging curves of the Zn||MnO_2 cells with (a) UiO-dcbdt-Zn@GF, (b) UiO-66@GF and (c) GF.

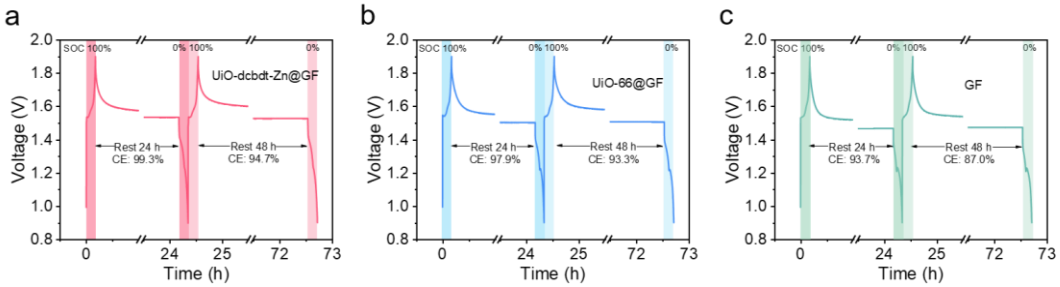

Figure S12. Evaluation of self-discharging level for Zn||MnO_2 cells rested at 100% stage of charge for 24 and 48 h.

Table S1. Comparison of cycling performance of Zn||MnO_2 full cells with MOF modified separators and Zn anodes.

Strategy	Materials	Current density ($A\ g^{-1}$)	Cycle number (N)	Capacity decay rate	Reference
Separator modification	**UiO-dcbdt-Zn@GF**	**1**	**2500**	**0.0060%**	**This work**
	UC/GF	1	3600	0.0077%	[10]
	MOF-NS/PAN	1	1500	0.0178%	[11]
	UiO-66-GF	1	1000	0.0150%	[12]
	GF-PFC-31	1.2	1000	0.0175%	[13]
	GF-Bio-MOF-100	0.5	1000	0.0161%	[14]
	Modified separator	1	500	0.0787%	[15]
Artificial protective layer	WSe_2/ZIF@Zn	1	2000	0.0048%	[16]
	MOF-74	0.2	1000	0.0226%	[17]
	Zn-SQ-3d-coated Zn	1	660	0.0150%	[18]
	ZIF-7/Zn	0.7	600	0.0180%	[19]
	ZIF-L/Zn	0.5	250	0.0400%	[20]

References

[1] M. L. Foo, S. Horike, T. Fukushima, Y. Hijikata, Y. Kubota, M. Takata and S. Kitagawa, *Dalton Trans.*, 2012, **41**, 13791-13794.

[2] H. Zhong, S. Chen, Z. Jiang, J. Hu, J. Dong, L. H. Chung, Q. C. Lin, W. Ou, L. Yu and J. He, *Small*, 2023, **19**, 2207266.

[3] G. Q. Lai, Z. Jiang, H. Zhong, L. H. Chung, N. Li and J. He, *Chinese J. Struc. Chem.*, 2023, **42**, 100090.

[4] R. Chen, G. Zhang, H. Zhou, J. Li, J. Li, L. H. Chung, X. Hu and J. He, *Small*, 2024, **20**, 2305687.

[5] G. Kresse and J. Hafner, *Phys. Rev. B*, 1993, **47**, 558.

[6] G. Kresse and J. Hafner, *Phys. Rev. B*, 1994, **49**, 14251.

[7] J. P. Perdew, K. Burke and M. Ernzerhof, *Phys. Rev. Lett.*, 1996, **77**, 3865.

[8] G. Kresse and D. Joubert, *Phys. Rev. B*, 1999, **59**, 1758.

[9] P. E. Blöchl, *Phys. Rev. B*, 1994, **50**, 17953.

[10] P. Yang, K. Zhang, S. Liu, W. Zhuang, Z. Shao, K. Zhu, L. Lin, G. Guo, W. Wang and Q. Zhang, *Adv. Funct. Mater.*, 2024, **34**, 2410712.

[11] C.-Y. Liu, Y.-D. Wang, H. Liu, Q. Chen, X. Jiang, H. Jia and J.-P. Lang, *Compos. Part B-Eng.*, 2024, **272**, 111227.

[12] Y. Song, P. Ruan, C. Mao, Y. Chang, L. Wang, L. Dai, P. Zhou, B. Lu, J. Zhou and Z. He, *Nano-Micro Lett.*, 2022, **14**, 218.

[13] R. Li, L. Pan, Z. Peng, N. Zhao, Z. Zhang, J. Zhu, L. Dai, L. Wang and Z. He, *J. Energy Chem.*, 2024, **93**, 213-220.

[14] R. Li, B. Yan, Z. Chen, Z. He and J. Yang, *J. Energy Chem.*, 2025, **25**, 01043.

[15] Y. Chen, C. Gao, J. Li, X. Liu, B. Zhou, J. Guo and C. Yu, *J. Energy Storage*, 2024, **103**, 114442.

[16] H. Wang, P. Wang, K. Yu, X. Wang, J. Cao, P. Jia, Y. Yuan and C. Liang, *Chem. Eng. J.*, 2024, **485**, 149544.

[17] D. Bi, T. Zhao, Q. Lai, J. Zhao and S. A. Grigoriev, *J. Alloy. Compd.*, 2024, **1002**, 175448.

[18] H. Lv, J. Wang, X. Gao, Y. Wang, Y. Shen, P. Liu, G. Wang, L. Chen and T. Gu, *ACS Appl. Mater. Interfaces*, 2023, **15**, 47094-47102.

[19] H. Yang, Z. Chang, Y. Qiao, H. Deng, X. Mu, P. He and H. Zhou, *Angew. Chem. Int. Ed.*, 2020, **132**, 9463-9467.

[20] W. He, T. Gu, X. Xu, S. Zuo, J. Shen, J. Liu and M. Zhu, *ACS Appl. Mater. Interfaces*, 2022, **14**, 40031-40042.